

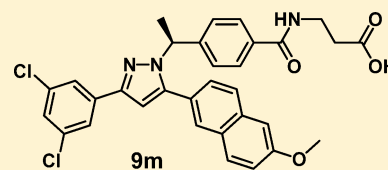
# Discovery of a Novel Glucagon Receptor Antagonist *N*-[(4-((1*S*)-1-[3-(3, 5-Dichlorophenyl)-5-(6-methoxynaphthalen-2-yl)-1*H*-pyrazol-1-yl]ethyl)phenyl)carbonyl]- $\beta$ -alanine (MK-0893) for the Treatment of Type II Diabetes

Yusheng Xiong,\* Jian Guo, Mari R. Candelore, Rui Liang, Corey Miller, Qing Dallas-Yang, Guoqiang Jiang, Peggy E. McCann, Sajjad A. Qureshi, Xinchun Tong, Shiyao Sherrie Xu, Jackie Shang, Stella H. Vincent, Laurie M. Tota, Michael J. Wright, Xiaodong Yang, Bei B. Zhang, James R. Tata, and Emma R. Parmee

Discovery and Preclinical Sciences, Merck Research Laboratories, P.O. Box 2000, Rahway, New Jersey 07065, United States

## Supporting Information

**ABSTRACT:** A potent, selective glucagon receptor antagonist **9m**, *N*-[(4-((1*S*)-1-[3-(3,5-dichlorophenyl)-5-(6-methoxynaphthalen-2-yl)-1*H*-pyrazol-1-yl]ethyl)phenyl)carbonyl]- $\beta$ -alanine, was discovered by optimization of a previously identified lead. Compound **9m** is a reversible and competitive antagonist with high binding affinity ( $IC_{50}$  of 6.6 nM) and functional cAMP activity ( $IC_{50}$  of 15.7 nM). It is selective for glucagon receptor relative to other family B GPCRs, showing  $IC_{50}$  values of 1020 nM for GIPR, 9200 nM for PAC1, and >10000 nM for GLP-1R, VPAC1, and VPAC2. Compound **9m** blunted glucagon-induced glucose elevation in hGCGR mice and rhesus monkeys. It also lowered ambient glucose levels in both acute and chronic mouse models: in hGCGR ob/ob mice it reduced glucose (AUC 0–6 h) by 32% and 39% at 3 and 10 mpk single doses, respectively. In hGCGR mice on a high fat diet, compound **9m** at 3, and 10 mpk po in feed lowered blood glucose levels by 89% and 94% at day 10, respectively, relative to the difference between the vehicle control and lean hGCGR mice. On the basis of its favorable biological and DMPK properties, compound **9m** (MK-0893) was selected for further preclinical and clinical evaluations.



## INTRODUCTION

Glucagon acts on its receptor in the liver to stimulate gluconeogenesis and glycogenolysis and thus increasing hepatic glucose production (HGP). As a major counterregulatory hormone to insulin, glucagon plays an important role in maintaining blood glucose homeostasis.<sup>1</sup> An inappropriately high rate of HGP is the predominant cause of fasting hyperglycemia and a major contributor to the postprandial hyperglycemia characteristic of type 2 diabetes.<sup>2</sup> Studies in type 2 diabetic subjects have demonstrated a causal role for glucagon in promoting excessive glucose production.<sup>3</sup> Glucagon-neutralizing antibodies,<sup>4</sup> glucagon receptor antisense oligonucleotides,<sup>5</sup> and peptide glucagon antagonists<sup>6</sup> all have been shown to be effective in animal models of diabetes, demonstrating the potential therapeutic value of suppressing the glucagon signaling pathway.<sup>7</sup>

There have been many reports detailing efforts to identify a small molecule glucagon receptor antagonist (GRA) as a potential oral treatment for type 2 diabetes, and much of the earlier work was reviewed by DeMong<sup>8</sup> in 2008. Early examples of GRA scaffolds such as a tetrasubstituted quinoxaline,<sup>9</sup> catechole derivatives,<sup>10</sup> a triaryl imidazole,<sup>11</sup> a phenol-containing alkylidene hydrazide,<sup>12,13</sup> and a tetrasubstituted thiophene<sup>14</sup> have not been followed up with further reports. One important early GRA is Bay 27-9955, which was

reported<sup>15</sup> in 2001 to have demonstrated an acute effect in blocking glucagon-induced glucose increase in healthy volunteers.

The  $\beta$ -alanine acid containing urea **1**,<sup>16a,b</sup> first published in a patent application in 2000 by Novo Nordisk and Agouron researchers, was derived from a screening hit. It has been a starting point for a large number of new designs leading to improved potency, DMPK properties, and identification of further advanced compounds. Changes in *N*-substitution groups in urea **1** led to compounds with improved PK properties<sup>16c,17</sup> and in vivo activity.<sup>18</sup> Various scaffold changes replacing the urea core in **1** from different laboratories have been reported in patent applications<sup>19</sup> and literature,<sup>20</sup> including a compound currently in clinical investigation<sup>21a</sup> which was likely derived from designs based on urea **1**.<sup>21b-d</sup>

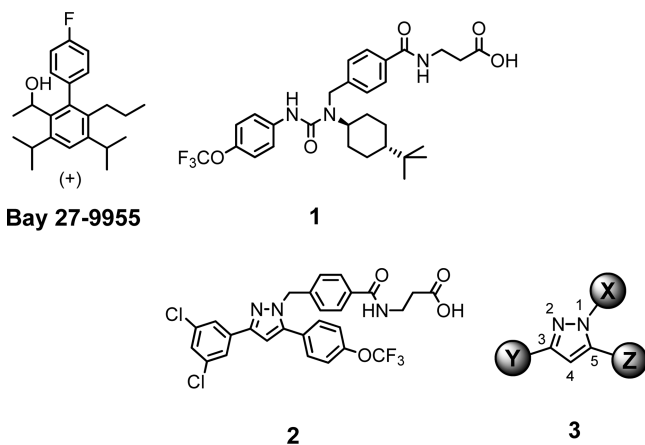
It was recognized by several groups that urea **1** can be considered as a molecule with three pharmacophores ( $\beta$ -alanine acid, 4-CF<sub>3</sub>O-Ph, and *t*-But-cyclohexyl) connected by the urea core. The starting point for this study, compound **2**,<sup>22</sup> had been designed based on the urea **1** with a pyrazole as replacement of the urea core. Other urea replacements reported are 2-aminothiazole,<sup>17</sup> biarylamine,<sup>23</sup> and  $\alpha$ -aryloxy amide com-

Received: April 24, 2012

Published: June 18, 2012

pounds,<sup>23</sup> retaining the  $\beta$ -alaninebenzamide plus aryl or alkyl groups projecting from the core, and these structures further supported the three-pharmacophore hypothesis.

One critical element in pharmacophore X in **3** is a properly positioned carboxylic acid or acid isostere. Extensive work, both in-house<sup>24</sup> and reported in literature,<sup>16b,23</sup> indicated that a  $\beta$ -alanine acid side chain is the group that best offers a proper balance of potency, DMPK, and physical properties. An aminotetrazole, for example, is a good replacement of  $\beta$ -alanine acid in terms of in vitro activity and selectivity, but compounds containing an aminotetrazole moiety tend to have poor oral bioavailability. The objective of the study reported below was the optimization of pharmacophores Y and Z in an effort to increase potency and improve selectivity over off-targets such as CYP and hERG. This lead optimization effort resulted in the discovery of two compounds that advanced to clinical studies. The identification of the first clinical candidate, **9m** (MK-0893), is detailed in this article.



## SYNTHESIS

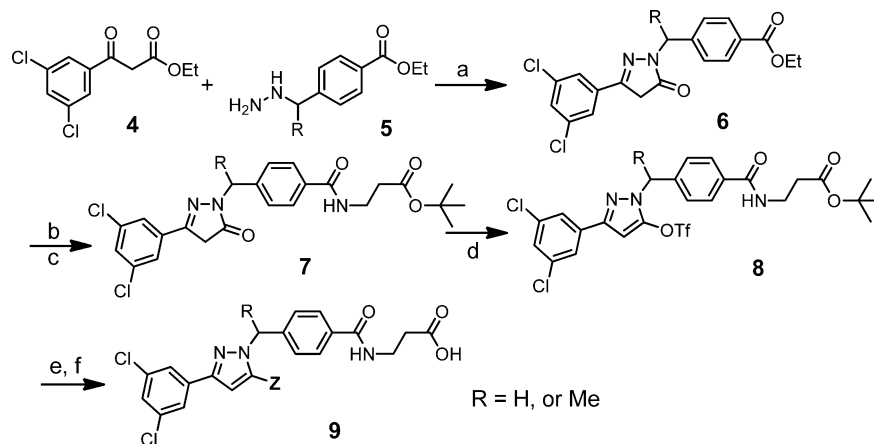
Compound **2** and a number of its analogues were synthesized<sup>22</sup> via condensation of 1,3-diketones with substituted hydrazines and subsequent cyclization, a reaction that produced a variable ratio of two regioisomeric 1,3,5-trisubstituted pyrazoles.

However, this pyrazole construction strategy did not prove suitable for SAR studies aimed at efficiently exploring the 3 and 5-positions as it requires incorporation of both the Y and Z groups into the requisite diketones at the very beginning of the synthetic sequence and it produces a mixture of regioisomers that requires separation. Therefore, we sought to develop a modular synthetic route that would allow incorporation of either the Y or Z group at the end of the synthetic sequence.

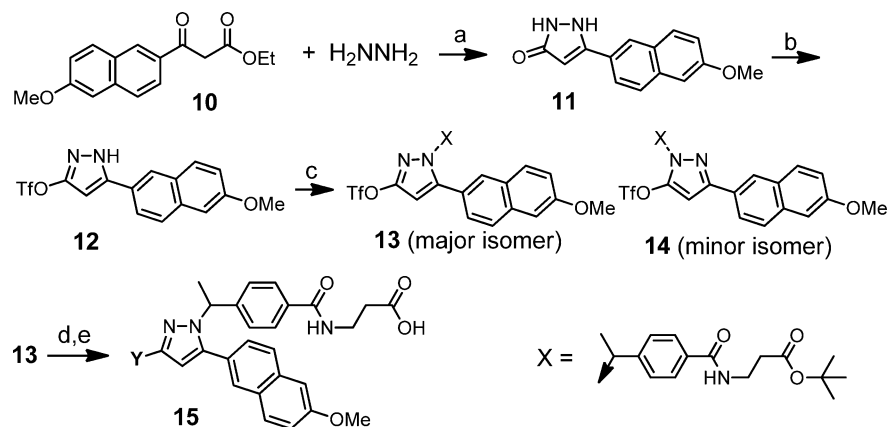
A regiospecific synthetic route to 1,3,5-trisubstituted pyrazole was developed based on a modification of a previously reported<sup>25</sup> pyrazole synthesis and is outlined in Scheme 1. The synthetic sequence started with the condensation of the appropriately substituted hydrazine **5** with the readily available  $\beta$ -ketoester **4** to give regioselectively the 1,3-substituted pyrazolinone **6**. Next, the protected  $\beta$ -alanine was installed to give compound **7**. Treatment of the pyrazolinone **7** with triflic anhydride afforded triflate **8** in good yield, with the reaction tolerating the fully elaborated side chain at the pyrazole-N-1 position. Pharmacophore Z was then incorporated via a Suzuki–Miyaura coupling of the pyrazole-5-triflate **8** with boronic acid Z-B(OH)<sub>2</sub>. Subsequent deprotection with trifluoroacetic acid afforded the desired compounds in good yields. Given the ease of access to the requisite starting materials, this regiospecific and high yielding route to pyrazole scaffold **3** allowed for rapid parallel synthesis of analogues for the optimization of the pharmacophore Z in terms of potency and off-target activities.

For the optimization of the pharmacophore Y, we further modified the synthetic route so that the Y group could be incorporated near the end of synthetic sequence. The synthesis of the pyrazolinone **11** started with ketoester **10** having the desired Z group, the 6-methoxynaphthyl, as illustrated in Scheme 2. The side chain X was installed via N-alkylation on the pyrazole triflate **12** with the expectation that selective N-alkylation might lead to a trisubstituted pyrazole with the triflate group at the pyrazole-3 position (regioisomer **13**). In the event, base-catalyzed alkylation of pyrazoles with alkyl halides gave mixtures of regioisomers depending on the reaction conditions<sup>27</sup> and, in the case of **12**, also led to a significant hydrolysis of the triflate group. Alternate conditions employing the milder Mitsunobu coupling with the corre-

Scheme 1. Synthetic Route for Studying SAR at Pyrazole 5-Position (Method A)<sup>a</sup>



<sup>a</sup>Conditions: (a) HOAc, reflux, 4 h, 66% yield; (b) NaOH; (c)  $\beta$ -alanine *t*-butylester, PyBOP, TEA, 75% yield over two steps; (d) triflic anhydride, TEA/THF,  $-78$ – $0$  °C, 93% yield; (e) Z-B(OH)<sub>2</sub>, Pd(PPh<sub>3</sub>)<sub>4</sub>, TEA, DME, microwave (100 °C, 10 min); (f) TFA/DCM, 95% yield over two steps. Yields were from the synthesis of **9m**.

Scheme 2. Synthetic Route for Studying SAR at Pyrazole 3-Position (Method B)<sup>a</sup>

<sup>a</sup>Conditions: (a) HOAc, reflux, 3 h, 86% yield; (b) triflic anhydride, TEA/THF,  $-78-0$  C, 46% yield; (c) X-OH, PPh<sub>3</sub>, DIAD, yields 49% (**13**) and 31% (**14**); (d) Y-B(OH)<sub>2</sub>, PdCl<sub>2</sub>(dppf), Cs<sub>2</sub>CO<sub>3</sub>, toluene, microwave (140 °C, 10 min); (e) TFA/DCM, 25% yield over two steps. Yields were from the synthesis of the racemic **15c**.

Table 1. GCGR and GIPR Activities of Pyrazole 9

compd	R	Z	GCGR binding <sup>a</sup>	GCGR cAMP <sup>a</sup>	GIPR <sup>b</sup> cAMP <sup>a</sup>
<b>2</b>	H	4-CF <sub>3</sub> O-Ph	86.2 ± 38.7	113.8 ± 43.4	6277 ± 2659
<b>9a</b>	H	2-CF <sub>3</sub> O-Ph	527.5		
<b>9b</b>	H	3-CF <sub>3</sub> O-Ph	233.6	238.0 ± 24.0	
<b>9c</b>	H	3-Cl, 4-PrO-Ph	37.9 ± 14.4	100.7 ± 47.8	3370
<b>9d</b>	H	naph-2-yl	60.6	58.5 ± 18.2	4337
<b>9e</b>	H	6-MeO-naph-2-yl	15.6 ± 5.5	90.9 ± 23.8	
<b>9f</b>	H	5-CF <sub>3</sub> O-naph-2-yl	40.5	114.2 ± 22.3	1984
<b>9g</b>	H	6-CF <sub>3</sub> O-naph-2-yl	8.1 ± 2.3	30.2 ± 2.2	711
<b>9h</b>	H	7-CF <sub>3</sub> O-naph-2-yl	64.2	189.0 ± 8.5	
<b>9i</b>	H	8-CF <sub>3</sub> O-naph-2-yl	121.5	239.8 ± 4.0	
<b>9j</b>	Me	4-CF <sub>3</sub> O-Ph	100.3	77.5 ± 16.8	
<b>9k</b>	Me	3-Cl, 4-PrO-Ph	16 ± 5.6	64.8 ± 49.3	478
<b>9m</b>	(S)-Me	6-MeO-naph-2-yl	6.6 ± 3.5	15.7 ± 5.4	1019 ± 275
<b>9n</b>	(R)-Me	6-MeO-naph-2-yl	728.3 ± 787.6	298.0	
<b>9p</b>	(S)-Me	6-CF <sub>3</sub> O-naph-2-yl	2.5 ± 1.1	11.9 ± 0.9	307 ± 48
<b>9q</b>	(R)-Me	6-CF <sub>3</sub> O-naph-2-yl	16.6 ± 3.7	32.6 ± 7.0	1134
<b>9r</b>	(S)-Me	6-CF <sub>3</sub> -naph-2-yl	10.7 ± 11.3	14.1 ± 6.5	378
<b>9s</b>	(S)-Me	6-Cl-naph-2-yl	7.5 ± 8.3	12.5 ± 3.6	795
<b>9t</b>	(S)-Me	6-Me-naph-2-yl	4.6 ± 1.9	7.5 ± 1.3	753
<b>9u</b>	(S)-Me	6-iPr-naph-2-yl	4.3 ± 0.6	13.3 ± 2.2	431
<b>9v</b>	(S)-Me	6-EtO-naph-2-yl	8.1 ± 3.5	23.6 ± 7.9	885
<b>9w</b>	Me	6-cyclohexyl-Ph	337.4	362.0	

<sup>a</sup>Activities are IC<sub>50</sub> in nM (mean ± SD),  $N \geq 2$  when SD is presented. <sup>b</sup>Functional assay in CHO cells expressing human GIPR, measuring cAMP production.

sponding benzyl alcohol proceeded in good overall yield and produced the desired triflate **13** as the major regioisomer. Compared to the pyrazole-5-triflate **8**, the pyrazole-3-triflate **13** was much less reactive in palladium-catalyzed coupling reactions.<sup>28</sup> After a very limited optimization effort, we settled on the coupling conditions shown in Scheme 2, which gave about 25% yield of the product after removal of the Boc group. In spite of this low yielding step at the end of synthesis sequence, the synthetic route of Scheme 2 was still cost-

effective and expedient for SAR exploration at the pyrazole 3-position. One gram-scale synthesis of intermediate **13** would allow synthesis of >30 compounds with different Y groups in a parallel synthesis in milligram scale. Any compounds of interest could then be scaled-up for further characterization and in vivo studies using the route outlined in Scheme 1.

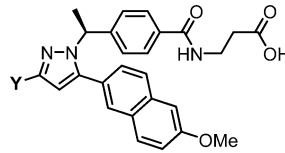
The hydrazines **5** used in Scheme 1 were synthesized by reductive amination of *tert*-butyl carbamate with ethyl 4-acylbenzoate (R = Me) or 4-formylbenzoate (R = H). The

racemate (R = Me) were resolved by chiral column chromatography and subsequent removal of the Boc group gave the enantiomeric hydrazine as their corresponding salt. The stereochemistry was established by converting **5** (R = Me) to its benzoylhydrazide and comparing to the compound of known stereochemistry.<sup>29</sup> For large-scale preparation of hydrazine **5** (R = Me), an asymmetric synthesis was developed based on enantioselective hydrogenation of *N*-alkoxycarbonyl hydrazones.<sup>30</sup> The boronic acids used in Schemes 1 and 2 were either commercially available or synthesized as described in detail in the Experimental Section.

## RESULTS AND DISCUSSION

Compounds in this report were first assayed in a receptor binding assay using a membrane preparation from a CHO cell line expressing the human GCGR (CHO hGCGR). Inhibition of binding between <sup>125</sup>I-glucagon and the GCGR was expressed as an IC<sub>50</sub> for compounds listed in Tables 1 and 2. The

**Table 2. GCGR and GIPR Activities of Pyrazole 15**



compd	Y	GCGR binding <sup>a</sup>	GCGR cAMP <sup>a</sup>	GIPR <sup>b</sup> cAMP <sup>a</sup>
15a	CF <sub>3</sub>	15.3 ± 5.6	63.1 ± 30.9	
15b	<i>t</i> -Bu	81.8	108.0	
15c	2,5-Cl, Cl-Ph	7.5 ± 1.2	11.5 ± 4.5	1844
15d	3,4-Cl, Cl-Ph	5.2 ± 1.5	15.8 ± 4.1	2419 ± 1203
15e	3-Cl, 5-CF <sub>3</sub> -Ph	1.9 ± 0.9	5.7 ± 1.9	1336
15f	3-Cl, 5-MeO-Ph	14.8 ± 4.0	67.9 ± 34.2	4996
15g	3-Cl, 5-PrO-Ph	6.9 ± 0.14	47.2 ± 12.0	2056
15h	2-Me, 5-CF <sub>3</sub> -Ph	9.3 ± 3.8	27.4	1684
15i	2-F, 5-CF <sub>3</sub> -Ph	4.1 ± 2.4	12.3 ± 5.6	933 ± 223

<sup>a</sup>Activities are IC<sub>50</sub> in nM (mean ± SD), N ≥ 2 when SD is presented.

<sup>b</sup>Functional assay in CHO cells expressing human GIPR, measuring cAMP production.

antagonist activity of compounds which exhibited good binding to the GCGR was confirmed in a functional assay using the CHO hGCGR cell line in the presence of glucagon. Inhibition of glucagon induced cAMP production by the compounds was expressed as an IC<sub>50</sub> in "GCGR cAMP" in Tables 1 and 2.

Previously reported structure–activity relationship studies on pyrazole **2**<sup>22</sup> and urea **1**<sup>16</sup> indicated that both the 4-trifluoromethoxyphenyl and 3, 5-dichlorophenyl served as potent pharmacophore Y moieties (position 3 of the pyrazole **2**, and as the left side N substitutions in the urea **1**), and these small aromatics provided a good starting point to explore the SAR of pharmacophore Z (pyrazole-5 position). A large number of analogues of generic structure **9** were synthesized from triflate **8** using method A as described above (R = H, CH<sub>3</sub>).

Table 1 highlights the important SAR features of pharmacophore Z. Unlike the urea series, the 4-*t*-butyl cyclohexyl, and 4-cyclohexylphenyl groups were not preferred groups for pharmacophore Z in the pyrazole series. Pyrazole analogues containing a 4-*t*-butyl cyclohexyl group (compound **3** in ref 22, and compound **9w**) were only moderately active, in contrast to compounds with small aromatic substituents at the

pyrazole-5 position. Aryl groups at the pyrazole 5-position showed a strong preference for para- and meta- substitution. For example, *para*-trifluoromethoxy analogue **2** (4-CF<sub>3</sub>O-phenyl) was 6-fold more potent than its ortho isomer **9a** (2-CF<sub>3</sub>O-phenyl). Meta, para-disubstituted compounds were more potent in the binding assay, as exemplified by compound **9c** (3-Cl, 4-PrO-phenyl), which showed an IC<sub>50</sub> of 38 nM in binding and 100 nM in functional cell assays. Attempts to bridge the meta- and para- groups into a ring in order to rigidify the propoxy group led to the substituted naphthalenes, which showed some increases in potency. Naphthalene (**9d**), and particularly 6-MeO-naphthalene (**9e**), showed improved binding activity as well as less than 100 nM functional activity in cAMP assay.

To fully explore the SAR of the substituents on the naphthalene group, the four regioisomeric naphthyl-2-boronic acids substituted with a CF<sub>3</sub>O group at positions 5, 6, 7, and 8 were synthesized, following the route developed by Schlosser and co-workers using the Diels–Alder cyclization of furan with in situ generated benzyne.<sup>31</sup> Activities of compounds **9f**, **9g**, **9h**, and **9i** clearly demonstrated the preference for the 2,6-substitution pattern on the naphthalene ring, with compound **9g** showing the highest binding activity (8 nM) and cAMP functional activity (30 nM) among the regioisomers.

Previous work<sup>32</sup> investigating *N*-indane substituted urea GRAs indicated that glucagon binding activity could be very sensitive to the stereochemistry at the indane carbon to which the urea nitrogen was attached. In the present series, substitution of the benzylic position of pyrazole lead compound **2** with a methyl group to give **9j** did not lead to any increase in binding affinity. Moreover, the two enantiomers of **9j** showed essentially the same activity when resolved (data not shown). In the case where a naphthalene was employed as the pharmacophore Z, the SAR at the benzylic position of pharmacophore X became more sensitive to substitution. The addition of a methyl group with an *S*- configuration (**9m**, **9p**) increased binding and functional activities of the compounds by more than 2-fold relative to their *des*-methyl analogues (**9e** and **9g**). The differences between (*S*)- and (*R*)- enantiomers ranged from 6- to 110-fold (**9m** vs **9n** and **9p** vs **9q**). Thus, the combination of a 2,6-disubstituted naphthalene as pharmacophore Z and the introduction of the benzylic methyl group afforded pyrazoles showing high binding affinities. Many potent compounds such as **9m**, **9s**, **9t**, **9u**, and **9v** were identified and thus increased the chance of identifying a suitable development candidate that was free of undesired off-target activities.

While a broader survey of SAR at the pyrazole-3 position had led us to focus on the small neutral groups in this position, focused libraries with 6-CH<sub>3</sub>O- and 6-CF<sub>3</sub>O-naphthalene at the pyrazole-5 position were prepared (Scheme 2) in order to further optimize pharmacophore Y. Table 2 lists a few compounds made with intermediate **13** (6-MeO-naphthalene at pyrazole 5-position) that highlight the SAR for pharmacophore Y.

Both small aliphatic and aromatic groups at the pyrazole-3 position were tolerated. Compounds with small aryl groups were slightly more active and, unlike pharmacophore Z, their activities were less sensitive to the regiochemistry of substitution on the pyrazole-3 aryl group, as exemplified by compounds **9e**, **15c**, and **15d**. Another observed SAR trend was the preference for a 5-CF<sub>3</sub> substitution on the aryl groups as found in compounds **15e**, **15h**, and **15i**, which were among the most potent compounds in this series.

Before extensive *in vivo* studies were carried out, compounds of interest were counterscreened against related targets and against selected off-targets such as ion channels important for cardiac functions. Close attention was paid to other related family B GPCRs such as GLP-1R and GIPR (glucose-dependent insulinotropic peptide receptor) because of their roles in insulin secretion. Receptor functional assays were set up to monitor compounds' antagonist activities at these receptors. For the pyrazole GCGR antagonist series, the selectivity against other related family B GPCRs (GLP-1R, VPAC1, and VPAC2) was generally very good except for GIPR. Activity against the GIPR was then used as a filter to select compounds for further profiling. Among compounds with different pyrazole 5-substitutions, compounds **9p**, **9r**, **9u**, and **9v** were very potent against the GCGR but not as selective as **9m** against the GIPR. In addition, compounds **9p** (6-CF<sub>3</sub>O-naphthalene) and **9r** (6-CF<sub>3</sub>-naphthalene) also showed hERG potassium channel (MK-499 binding) activity ( $IC_{50} < 1.2 \mu M$ ). On the other hand, compound **9t** (6-CH<sub>3</sub>-naphthalene) and **9m** (6-CH<sub>3</sub>O-naphthalene) did not bind to hERG ( $IC_{50} > 10 \mu M$ ), but unfortunately compound **9t** showed moderate activity in a diltiazem-sensitive calcium channel ( $IC_{50} 2.1 \mu M$ ) assay.

Many compounds listed in Table 2 were potent GCGR antagonists and selective with respect to GIPR, and compounds **15c**, **15d**, **15e**, and **15i** were all equal or more potent than compound **9m**. Further profiling in counterscreens revealed that compound **15c** was active against other family B GPCR such as GLP-1R ( $IC_{50} 8.2 \mu M$ ) and VPAC2 ( $IC_{50} 2.6 \mu M$ ). It also showed moderate ion channel activities ( $IC_{50} 9.7 \mu M$  for hERG, and  $8.8 \mu M$  for diltiazem-sensitive calcium channel) that may lead to adverse cardiac effects. Compound **15d** was equally potent against GCGR compared to **9m** but showed less selectivity with regards to VPAC2 ( $IC_{50} 1.7$  vs  $12.8 \mu M$ ). Compound **15e**, when compared to **9m**, was nearly 3-fold more potent against the GCGR and more selective with regards to the GIPR. Unfortunately compound **15e** also showed moderate activity at the GLP-1R ( $IC_{50} 3.3 \mu M$ ) and VPAC2 ( $IC_{50} 2.6 \mu M$ ) and therefore was not profiled further. Compound **15i** was very potent against the GCGR and also very selective with regards to other family B GPCRs. When further profiled in counterscreens and ADME studies, **15i** showed the same selectivity profile and similarly favorable DMPK properties as **9m**. While compound **9m** was selected as clinical candidate, **15i** was extensively studied in various animal models to advance our understanding of glucagon receptor biology.<sup>33</sup>

The 3,5-dichlorophenyl and 6-methoxynaphthalene groups in **9m** seemed to possess the right balance of desired activity and off-target selectivity. Among the compounds listed in Tables 1 and 2, compound **9m** was the best overall in terms of off-target selectivity (Table 3). Upon incubation with human hepatocytes at 1 and  $10 \mu M$  for 48 h, compound **9m** did not increase CYP3A4 mRNA expression or CYP3A4-mediated testosterone  $6\beta$ -hydroxylase activity, and thus it was not an inducer of CYP3A4. Furthermore, compound **9m** produced no treatment-related changes in assays evaluating cardiovascular effect in anesthetized dogs (up to 10 mpk IV, reaching drug exposure of  $125 \mu M$ ) and central nervous system effect in conscious mice ( $100 \mu M$  PO).

Compound **9m** is a competitive, reversible GCGR antagonist, as evidenced by Schild Analysis in CHO cells expressing the hGCGR (Figure 1). It dose dependently right-shifted the  $EC_{50}$  of glucagon without changing the maximum effect of glucagon. The binding of **9m** was fully reversible

Table 3. Activity Profile of Compound **9m**

glucagon receptor		$IC_{50}$ (nM) <sup>a</sup>
human		$15.7 \pm 0.54$
rhesus		55.5
dog		$104.5 \pm 62.8$
mouse		122
rat		$727 \pm 350$
other family B GPCR		$IC_{50}$ (nM) <sup>a</sup>
GIPR		1020
GLP-1R		>10000
PAC1		9200
VPAC1		11580
VPAC2		12800
ion channels		$IC_{50}$ (nM)
h-ERG <sup>b</sup>		>10000
L-type Ca <sup>2+</sup> <sup>c</sup>		>10000
Nav1.5 <sup>d</sup>		-7% @ $10 \mu M$
P450		$IC_{50}$ ( $\mu M$ ) <sup>e</sup>
Cyp3A4		$60 \pm 9.6$
Cyp2D6		>100
Cyp2C8		$2.7 \pm 0.2$
Cyp2C9		$14 \pm 1.8$
Cyp1A2		$92 \pm 5.0$
Cyp2B6		$23 \pm 2.0$
Cyp2E1		>100

<sup>a</sup>Functional assay (ref 34)] in CHO cells expressing human (if not specified) receptors, measuring compounds' inhibition of cAMP production. Activities are  $IC_{50}$  in nM (mean  $\pm$  SD),  $N \geq 2$  when SD is presented. <sup>b</sup>IKr binding assay, ref 35a. <sup>c</sup>Binding assay with [<sup>3</sup>H]-diltiazem, ref 35b. <sup>d</sup>Reference 35c. <sup>e</sup>Human liver microsome P450 marker enzyme activities with testosterone  $6\beta$ -hydroxylation for 3A4, dextromethorphan *O*-demethylation for 2D6, paclitaxel  $6\alpha$ -hydroxylation for 2C8, diclofenac 4'-hydroxylation for 2C9, phenacetin *O*-deethylation for 1A2, bupropion hydroxylation for 2B6, and chlorzoxazone  $6\beta$ -hydroxylation for 2E1.

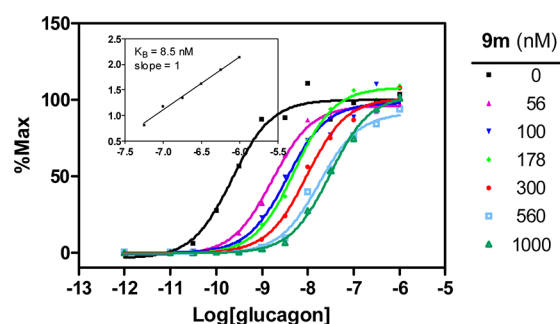


Figure 1. Schild analysis of compound **9m** in CHO cell expressing hGCGR. Glucagon  $EC_{50}$  in this cell line was  $0.22 \pm 0.02$  nM.

within the 30 min of the equilibration period used in the assay. Linear transformation of the data (insert in Figure 1) yielded a straight line with a slope of 1 (Hill coefficient,  $n_h$ ), and a  $K_B$  of 8.5 nM.

Concern over potential metabolic instability of compound **9m** due to the 6-methoxynaphthalene group was quickly dispelled by the results of pharmacokinetic studies in several species, as shown in Table 4. Compound **9m** was characterized by low clearance, with a  $Cl_p$  of 7.5, 0.18, and  $2.5 \text{ mL}/\text{min}/\text{kg}$ , in rat, dog, and rhesus monkey, respectively. The elimination half-life was species-dependent, varying from 5.9 h (rat) to 17 h (dog). The oral bioavailability ( $F$ ) of **9m** was  $\sim 43\%$  in rat,  $43\%$

**Table 4. Mean Pharmacokinetic Parameters of 9m in Nonclinical Species**

parameter <sup>a</sup>	mouse <sup>b</sup>	rat	dog	monkey
dose IV/PO (mg/kg)	1/2	2/2	0.5/0.5	0.5/2
Cl <sub>p</sub> (mL/min/kg)	5.4	7.5	0.18	2.5
Vd <sub>ss</sub> (L/kg)	1.6	2.1	0.27	0.9
T <sub>1/2</sub> (h)	5.2	5.9	17	5.7
F <sub>oral</sub> (%) <sup>c</sup>	37	43	43	57
nAUC <sub>oral</sub> (μM·h/(mg/kg)) <sup>c</sup>	2.0	1.7	66	6.4

<sup>a</sup>Cl<sub>p</sub>, plasma clearance; Vd<sub>ss</sub>, volume of distribution at steady state; T<sub>1/2</sub>, half-life; F<sub>oral</sub>, oral bioavailability; nAUC, dose-normalized area under the plasma concentration versus time curve. <sup>b</sup>Parameters determined using blood concentrations. <sup>c</sup>In mice, oral pharmacokinetic properties were determined using a solution in DMSO:Tween80:water (5:10:85 by volume). In other species, oral pharmacokinetic properties were determined using a suspension in 0.5% aqueous methylcellulose vehicle.

in dog, and 57% in rhesus. Further studies indicated that compound **9m** was metabolically very stable, undergoing only minor metabolism in vitro and in vivo. In vivo disposition studies in bile duct cannulated rats and dogs using tritium-labeled **9m** indicated that elimination occurred almost exclusively via biliary excretion of the parent compound (Figure 1s, Supporting Information) and that compound **9m** was the only radioactive plasma component in both rat and dog at all the time points sampled (Figures 2s, 3s, Supporting Information). In vitro metabolism studies in liver microsomes and hepatocytes from rat, dog, monkey, and human using tritium-labeled **9m** revealed minor amounts of *O*-demethylation (M1), acyl glucuronide (M2) of **9m**, and acyl glucuronide of the benzoic acid (M3) derived from hydrolysis of the amide bond of **9m** (Figure 1s, Supporting Information). In all cases, the total metabolites represented <2% turnover in the in vitro incubations.

Plasma protein binding was also determined in vitro with the tritium-labeled **9m**. Compound **9m** was highly bound (>99%) to rat, dog, monkey, and human plasma proteins, and the unbound fraction could not be accurately determined.

In an acute glucagon challenge model in hGCGR mice,<sup>36</sup> compound **9m** was found to be active in blunting glucagon-induced glucose excursion, Figure 2. When dosed orally at 3,

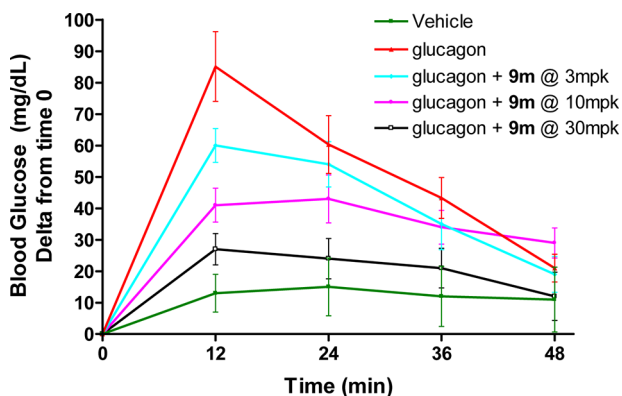


**Figure 2.** Effect of **9m** on glucagon-induced glucose level in hGCGR mice. Compound **9m** was dosed orally at one hour prior to IP glucagon administration (15 μg/kg). Data represents mean ± SEM (*n* = 8–10). Drug levels at 60 min were determined 0.26/1.15/2.88 μM for 3/10/30 mpk.

10, and 30 mpk one hour prior to a glucagon challenge (IP, 15 μg/kg), compound **9m** reduced glucose elevation relative to vehicle control by 30%, 56%, and 81%, respectively, as determined by AUC over a 0–24 min period (all with *p* < 0.05 vs the glucagon group). The drug levels were found to be 0.26, 1.15, and 2.88 μM for 3, 10, and 30 mpk dose groups, respectively. In an ex vivo study using an hGCGR mouse perfused liver model,<sup>37</sup> the glucagon-induced glycogenolysis (determined by following the <sup>13</sup>C NMR signal of glycogen derived from [2-<sup>13</sup>C]pyruvate in perfusate) was effectively inhibited by **9m** added to the perfusate (Figure 5s, Supporting Information). Compound **9m** inhibited glucagon-induced glycogenolysis by 12/44/66% at 0.1/0.3/1.0 μM initial concentration in perfusate and completely blocked glucagon-induced glycogenolysis at 3 μM. This experiment confirmed that compound **9m** acted in the liver by inhibiting hepatic glucose production.<sup>38</sup>

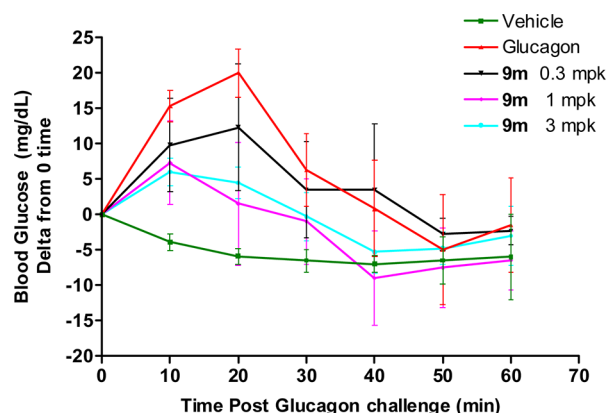
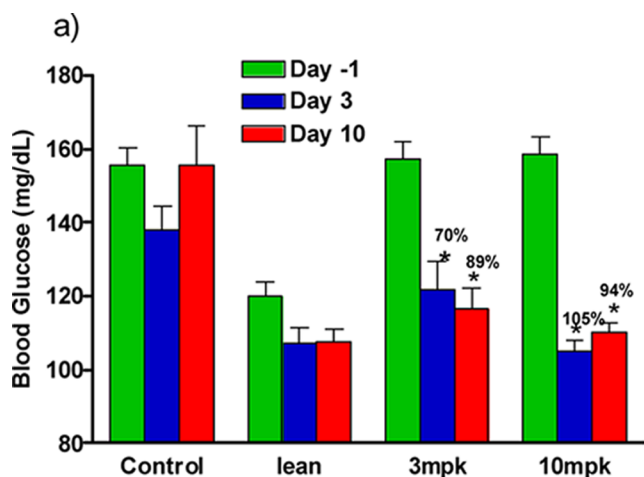


**Figure 3.** Effect of **9m** on glucagon-induced glucose level in rhesus. Compound **9m** was dosed to chair-restrained rhesus monkeys via a nasogastric tube at 0.3, 1, and 3 mpk four hours prior to an intramuscular glucagon challenge (15 μg/kg). Data represents mean ± SEM (*N* = 4). Drug levels at 4 h post dose were 0.1/0.3/0.74 mM at 0.3/1/3 mpk.

Compound **9m** was active against the rhesus monkey GCGR, showing an IC<sub>50</sub> of 56 nM in a cAMP assay with CHO cells expressing the rhesus GCGR. The compound was evaluated in vivo in a rhesus glucagon challenge model similar to that utilized in the hGCGR mouse. When compound **9m** was administered to chair-restrained rhesus monkeys via a nasogastric tube at 0.3, 1, and 3 mpk four hours prior to an intramuscular glucagon challenge (15 μg/kg), it significantly reduced the glucagon-induced glucose levels at 1 and 3 mpk with a 59 and 55% correction to the vehicle response. A nonstatistically effective dose was observed at 0.3 mpk (29% reduction). The mean plasma levels at the time of glucagon administration were 0.1, 0.3, and 0.7 μM at 0.3, 1.0, and 3.0 mpk, respectively.

Compound **9m** demonstrated efficacy in glucose lowering in a hGCGR ob/ob mice<sup>33</sup> in an acute model, Figure 4s, Supporting Information. Compared to vehicle control group, compound **9m** at 10 and 3 mpk oral doses lowered blood glucose level (AUC 0–6 h post dose) by 39%, 32% respectively. At 1 mpk, compound **9m** lowered glucose at 1 and 3 h but not at 6 h post dose. At 0.3 mpk, there was no effect at 1, 3, and 6 h time points. Compound **9m** was also efficacious in lowering ambient glucose level in a chronic setting using diet-induced obese hGCGR mice.<sup>39</sup> This group of



b) Plasma drug level, and blood glucagon, total GLP-1 level in control and treated hGCGR mice

	9m ( $\mu\text{M}$ )	Glucagon (pg/ml)	Total GLP-1 (pM)
Control		445 $\pm$ 55	46 $\pm$ 4
3 mpk	0.41~0.58	1274 $\pm$ 324	89 $\pm$ 11
10 mpk	0.82~1.50	2390 $\pm$ 477	88 $\pm$ 76

**Figure 4.** (a) Effect of chronic administration of **9m** on blood glucose in the DIO hGCGR mice. Compound was dosed in feed (high fat diet) for 11 days at 3 and 10 mpk ( $n = 11-15$ ). Numbers on bar represent % correction to lean group, \*  $p < 0.05$  vs respective controls. (b) Postprandial plasma drug levels were determined on day 5. Blood levels of glucagon and total GLP-1 were determined at day 11.

hGCGR mice on a high fat diet developed a mild degree of nonfasting hyperglycemia, hyperinsulinemia, and hyperglucagonemia and offered a good opportunity to evaluate the GCGR antagonists' efficacy in ambient glucose reduction. When dosed in feed (high fat diet S3282 from Bio-Serv) at 3 and 10 mpk per day, compound **9m** demonstrated a glucose lowering effect by day 3 and maintained lower glucose levels in the treatment groups throughout the duration of the study, Figure 4. At day 3, the glucose levels relative to the difference between the vehicle control group and lean group were reduced by 70% and 105% for the 3 and 10 mpk groups, respectively. At day 10, the corresponding glucose reductions were 89% and 94% for the 3 and 10 mpk groups, respectively. In this 10-day chronic treatment, the glucagon and GLP-1 levels were also increased relative to vehicle control group, a result of feedback upregulation of proglucagon expression. Glucagon levels were elevated by 1.5- and 2.6-fold in the 3 and 10 mpk groups, respectively. Total GLP-1 also increased by 2.1- and 4.0-fold in the 3 and 10 mpk groups, respectively. Note that these increases in glucagon were far less than the reported increase observed in the GCGR knockout mice ( $>100\times$ ).<sup>40</sup> In keeping with previously reported data, no gross morphological changes in pancreatic tissues were observed.<sup>39</sup>

## CONCLUSION

In summary, the development of a modular synthesis of 1,3,5-trisubstituted pyrazoles allowed thorough investigation of the SAR around the pyrazole 3- and 5- positions. Two key findings of the SAR studies in this pyrazole GCGR antagonist series were the potency enhancing effect of 6-substituted naphth-2-yl groups at the pyrazole 5-position, and the incorporation of a chiral methyl group at the benzylic position off the pyrazole-N-1. Consequently a large number of potent GCGR antagonists were synthesized; among them, compound **9m** was further profiled due to its balanced potency and selectivity profile.

Compared with the initial lead compound **2** in this pyrazole series, compound **9m** showed increased potency on the GCGR (13-fold in binding, 7-fold in functional assay) and improved off-target selectivity profile, particularly in hERG channel binding activity ( $IC_{50} >10 \mu\text{M}$  for **9m** vs  $5.1 \mu\text{M}$  for **2**). It is interesting to note that incorporation of  $\text{CF}_3$  group in the para (or pseudo para) position in pharmacophore Z was associated

with hERG channel activity:  $IC_{50}$  in hERG channel binding was  $<1.2 \mu\text{M}$  for compound **9p** and **9r**. Compound **9m** showed an improved selectivity in reversible binding to CYP3A4 but had moderate reversible inhibition of CYP2C8.

Compound **9m** is a reversible, competitive human GCGR antagonist with  $K_B$  of 8.5 nM. It is moderately active against the mouse, dog, and rhesus GCGRs but significantly less active at the rat GCGR. Compound **9m** is selective for the glucagon receptor relative to other family B GPCRs tested, GIPR ( $IC_{50}$ , 1020 nM), PAC1 ( $IC_{50}$ , 9200 nM), and GLP-1R/VPAC1/VPAC2 ( $IC_{50} >10000$  nM). Compound **9m** demonstrated acute efficacy in blunting glucagon-induced glucose elevation in hGCGR mouse and rhesus monkey models. In a hGCGR mice PD study, it reduced glucose levels (AUC 0–1 h post dose) by 56%, and 81% at 10 and 30 mpk oral doses, respectively. In a rhesus monkey PD study, it demonstrated 59% and 55% reduction in glucose level relative to vehicle group at 1 and 3 mpk oral doses, respectively.

Compound **9m** was also efficacious in lowering ambient glucose levels in hGCGR mice models. In a hGCGR ob/ob mice acute model, it reduced glucose level (AUC 0–6 h post dosing) by 32% and 39% at 3 and 10 mpk oral doses, respectively. In a subchronic study in hGCGR mice on a high fat diet, it reduced ambient glucose levels by 89% and 94% at 3 and 10 mpk doses, respectively, in feed at day 10.

In spite of having a 6-methoxynaphthalene group on the periphery, compound **9m** is actually very stable metabolically in vitro and in vivo. It has low clearance in preclinical species tested (Clp of 7.5, 0.2, and 2.5 mL/min/kg, in rats, dogs, and rhesus monkeys, respectively), and the major clearance route of compound **9m** is via biliary excretion as the parent compound. Except for moderate inhibition of CYP2C8 ( $IC_{50}$  2700 nM), compound **9m** does not inhibit major CYPs nor is it a CYP3A4 inducer.

Compound **9m** was well-tolerated in a five-week safety study in rat, with no treatment-related antemortem or postmortem findings at doses  $\leq 100$  mpk daily ( $C_{max}$  reached  $21.3 \pm 1.4 \mu\text{M}$ ). On the basis of the efficacy and good selectivity profile, compound **9m** was selected for further evaluation in preclinical safety species and entered into clinical studies for type II diabetes treatment.<sup>41a</sup> In a phase IIa study in diabetic patients, compound **9m**, at 200 and 1000 mg single doses, achieved

~59% and near maximal blockade of glucagon-induced glucose excursions, respectively.<sup>41b</sup> In a 12-week phase IIB clinical study<sup>41c</sup> in type II diabetic patients, compound **9m** demonstrated robust reduction from baseline level in fasting plasma glucose (−53 and −63 mg/dL) and HbA1c (−1.1 and −1.5%) at 60 and 80 mg qd doses, respectively ( $p < 0.001$ ), surpassing metformin at 1000 mg bid (−37 mg/dL and −0.8%,  $p < 0.001$ ).

## EXPERIMENTAL SECTION

**General Methods.** All commercial chemicals and solvents were reagent grade and were used without further purification unless otherwise specified. <sup>1</sup>H NMR spectra were recorded on a Varian InNova 500 MHz spectrometer. High resolving power accurate mass measurement electrospray (ES) mass spectral data were acquired by use of a Bruker Daltonics 7T Fourier transform ion cyclotron resonance mass spectrometer (FT-ICR MS). Low-resolution mass spectra were determined on a Micromass platform liquid chromatography–mass spectrometer (LC-MS), using a Waters Xterra MSC18 3.5  $\mu\text{m}$ , 50 mm  $\times$  3.0 mm column with a binary solvent system where solvent A was water and 0.05% trifluoroacetic acid (by volume) and solvent B was acetonitrile and 0.05% trifluoroacetic acid (by volume). The LC method used a flow rate of 1.0 mL/min with the following gradient:  $t = 0$  min, 90% solvent A;  $t = 3.75$  min, 2.0% solvent A;  $t = 4.75$  min, 2% solvent A;  $t = 4.76$  min, 90% solvent A;  $t = 5.5$  min, 90% solvent A. LC-MS HPLC method served as analysis of purity over a broad range, and all final compounds showed a single peak (>95% purity) using this analytical method. Preparative TLC was done on Analtech Uniplate: catalogue number 02015, silica gel GF, 20 cm  $\times$  20 cm, 2000  $\mu\text{m}$ .

**Preparation of {(1S)-1-[4-(Ethoxycarbonyl)phenyl]ethyl}hydrazinium Chloride (5, R = Me).** *Step 1.* A solution of *tert*-butyl carbazate (13.9 g, 105 mmol) and ethyl 4-acetylbenzoate (20.0 g, 104 mmol) in toluene (120 mL) was stirred at 80 °C overnight. *tert*-Butyl-2-[1-[4-(ethoxycarbonyl)phenyl]-ethylidene]-hydrazinecarboxylate separated as a crystalline solid (29.2 g, 92%) and was collected by filtration. HPLC/MS:  $m/z = 307.3$  (M+1)<sup>+</sup>. <sup>1</sup>H NMR (500 MHz, CDCl<sub>3</sub>)  $\delta$ : 1.43 (t,  $J = 7.0$  Hz, 3H), 2.24 (s, 3H), 1.58 (s, 9H), 4.41 (q,  $J = 7.0$  Hz, 2H), 7.79 (br s, 1H), 7.88 (d,  $J = 8.5$  Hz, 2H), 8.05 (d,  $J = 8.5$  Hz, 2H).

*Step 2.* In a N<sub>2</sub> filled round-bottomed flask, NaBH<sub>3</sub>CN (6.3 g, 100 mmol) and *tert*-butyl-2-[1-[4-(ethoxycarbonyl)phenyl]ethylidene]-hydrazinecarboxylate (29.2 g, 95.4 mmol) were dissolved in THF (200 mL). A solution of *p*-toluenesulfonic acid monohydrate (19.0 g, 100 mmol) in THF (50 mL) was slowly added via syringe pump in 10 h. The mixture was diluted with EtOAc (200 mL) and the suspension extracted with brine (150 mL). The organic phase was separated, dried (Na<sub>2</sub>SO<sub>4</sub>), and concentrated to give a white solid. The solid was taken in DMC (100 mL), and 1 N NaOH (100 mL) was added. The suspension was stirred vigorously at rt for 1 h and then diluted with DMC (100 mL). The organic phase was separated and washed with 1N HCl (2  $\times$  150 mL) and brine (2  $\times$  150 mL), dried (Na<sub>2</sub>SO<sub>4</sub>), and concentrated to approximately 50 mL. Product precipitated as white solid and was washed with hexane to yield 29 g (98%) of *tert*-butyl 2-[1-[4-(ethoxycarbonyl)phenyl]ethyl]hydrazinecarboxylate. HPLC/MS:  $m/z = 331.3$  (M + Na)<sup>+</sup>. <sup>1</sup>H NMR (500 MHz, CDCl<sub>3</sub>)  $\delta$ : 1.35 (d,  $J = 6.5$  Hz, 3H), 1.41 (t,  $J = 7.0$  Hz, 3H), 1.45 (s, 9H), 4.29 (m, 1H), 4.40 (q,  $J = 8.0$  Hz, 2H), 5.99 (br s, 1H), 7.44 (d,  $J = 8.0$  Hz, 2H), 8.03 (d,  $J = 8.0$  Hz, 2H).

The enantiomers were separated on ChiralPak AD column using EtOH/*n*-heptane (20%/80%). The fast eluting isomer was identified as (S)-enantiomer ( $[\alpha]_{\text{D}}^{20} = -120^\circ$  (c1.1, MeOH)), the slow eluting the (R)-enantiomer ( $[\alpha]_{\text{D}}^{20} = +122^\circ$  (c1.1, MeOH)). The absolute stereochemistry was established by converting the hydrazine to ethyl 4-[1-(2-benzoylhydrazino)ethyl]benzoate (Supporting Information) and comparison of optical rotation with that of the literature value.<sup>29</sup>

*Step 3.* *tert*-Butyl 2-[(1S)-1-[4-(ethoxycarbonyl)phenyl]ethyl]-hydrazinecarboxylate (14 g, 45 mmol) was treated with 50 mL of TFA–DCM–triisopropylsilane (20:20:1) at room temperature for 1 h.

The mixture was concentrated under reduced pressure, and the residue was dissolved in water (50 mL) and washed with DCM twice. The DCM was back extracted with water three times, and HCl (5N, 10 mL) was added to the combined water solution and concentrated to ~25 mL. CH<sub>3</sub>CN (50 mL) was added, and this was lyophilized to give 10.7 g (97%) of {(1S)-1-[4-(ethoxycarbonyl)phenyl]ethyl}-hydrazinium chloride. NMR (500 MHz, acetone-*d*<sub>6</sub>)  $\delta$ : 1.34 (t,  $J = 7.1$  Hz, 3H), 1.67 (d,  $J = 6.8$  Hz, 3H), 4.33 (q,  $J = 7.1$  Hz, 2H), 4.97 (q,  $J = 6.8$  Hz, 1H), 7.76 (d,  $J = 8.5$  Hz, 2H), 7.97 (d,  $J = 8.5$  Hz, 2H). MS C<sub>11</sub>H<sub>16</sub>N<sub>2</sub>O<sub>2</sub> calcd 208.12; obsd (M + 1) 209.19.

***tert*-Butyl N-[(4-[(1S)-1-[3-(3,5-Dichlorophenyl)-5-[[trifluoromethyl]sulfonyloxy]-1H-pyrazol-1-yl]ethyl]phenyl)carbonyl]- $\beta$ -alaninate (8, R = (S)-Me).** *Step 1.* A solution of ethyl (3,5-dichlorobenzoyl)acetate (3.0 g, 11.5 mmol) and {(1S)-1-[4-(ethoxycarbonyl)phenyl]ethyl}hydrazinium chloride (2.55 g, 10.4 mmol) was refluxed in HOAc (80 mL) for 4 h. The solvent was removed under reduced pressure and the residue taken up with ethyl acetate, washed with satd NaHCO<sub>3</sub> twice and brine, and dried over Na<sub>2</sub>SO<sub>4</sub>. Flash column chromatography (SiO<sub>2</sub>, 0–5% ethyl acetate in DCM gradient) gave 2.8 g (66%) of ethyl 4-[(1S)-1-[3-(3,5-dichlorophenyl)-5-oxo-4,5-dihydro-1H-pyrazol-1-yl]ethyl]benzoate (6, R = (S)-Me) as a colorless oil. <sup>1</sup>H NMR (500 MHz, CDCl<sub>3</sub>)  $\delta$ : 1.38 (t,  $J = 7.1$  Hz, 3H), 1.78 (d,  $J = 7.0$  Hz, 3H), 3.55 (d,  $J = 22.6$  Hz, 1H), 3.60 (d,  $J = 22.6$  Hz, 1H), 4.36 (q,  $J = 7.1$  Hz, 2H), 5.57 (q,  $J = 7.0$  Hz, 1H), 7.39 (t,  $J = 1.9$  Hz, 1H), 7.50 (d,  $J = 8.4$  Hz, 2H), 7.52 (d,  $J = 1.9$  Hz, 2H), 8.02 (d,  $J = 8.4$  Hz, 2H). MS C<sub>20</sub>H<sub>18</sub>Cl<sub>2</sub>N<sub>2</sub>O<sub>3</sub> calcd 404.07; obsd (M + 1) 405.20.

*Step 2.* Compound 6 (R = (S)-Me) (2.23 g, 5.50 mmol) was dissolved in MeOH–dioxane (1:1, 50 mL). A solution of NaOH (0.7 g/15 mL) was added. The mixture was heated to 60 °C for 1 h. This was acidified with 2N HCl (10 mL), and the solvent was removed and residue vacuum-dried to give a pale-yellow solid (mixture of product and NaCl). This solid was suspended in DMF (15 mL), followed with addition of DIEA (4.8 mL),  $\beta$ -alanine *tert*-butyl ester hydrochloride (3 g, excess). A solution of PyBOP (3.43 g, 6.6 mmol) in DMF (5 mL) was then added. After stirring at room temperature for 3 h, more PyBOP (1 g) was added, and the reaction mixture was stirred overnight. After addition of water (5 mL), the mixture was heated to 60 °C for 30 min. Ethyl acetate (150 mL) was added, and the organic layer was washed with 0.5 N HCl twice, 5% K<sub>2</sub>CO<sub>3</sub> twice, and brine twice. Evaporation of solvent gave an oily residue, which after flash column chromatography (SiO<sub>2</sub>, 0–30% ethyl acetate in DCM) afforded 2.1 g (75%) of *tert*-butyl N-(4-[(1S)-1-[3-(3,5-dichlorophenyl)-5-oxo-4,5-dihydro-1H-pyrazol-1-yl]ethyl]benzoyl)- $\beta$ -alaninate (7, R = (S)-Me) as a white solid. <sup>1</sup>H NMR (500 MHz, DMSO-*d*<sub>6</sub>)  $\delta$ : 1.37 (s, 9H), 1.78 (d,  $J = 7.1$  Hz, 3H), 2.45 (t,  $J = 7.0$  Hz, 2H), 3.42 (q,  $J = 7.0$  Hz, 2H), 5.56 (q,  $J = 7.1$  Hz, 1H), 5.99 (s, 1H), 7.30 (d,  $J = 8.3$  Hz, 2H), 7.47 (t,  $J = 1.0$  Hz, 1H), 7.73 (d,  $J = 8.3$  Hz, 2H), 7.76 (d,  $J = 1.9$  Hz, 2H), 8.43 (t,  $J = 5.6$  Hz, 1H), 11.34 (s, 1H). MS C<sub>25</sub>H<sub>27</sub>Cl<sub>2</sub>N<sub>3</sub>O<sub>4</sub> calcd 503.14; obsd (M + Na) 526.05.

*Step 3.* Compound 7 (R = (S)-Me) (2.05 g, 4.06 mmol) and TEA (1.7 mL, 12 mmol) were dissolved in THF (35 mL) at −78 °C. Triflic anhydride (1.1 mL, 6.2 mmol) was added. The cooling bath was removed, and the reaction mixture was stirred for 1 h. The reaction was quenched by adding ethyl acetate and water. The organic layer was washed with 0.5 N HCl twice and brine twice and dried over Na<sub>2</sub>SO<sub>4</sub>. Evaporation of solvent and flash column chromatography (SiO<sub>2</sub>, 0–10% ethyl acetate in DCM gradient) gave 2.4 g (93%) of *tert*-butyl N-{4-[1-(3-(3,5-dichlorophenyl)-5-[[trifluoromethyl]sulfonyloxy]-1H-pyrazol-1-yl]ethyl]-benzoyl}- $\beta$ -alaninate (8, R = (S)-Me) as a colorless dry film. <sup>1</sup>H NMR (500 MHz, CDCl<sub>3</sub>)  $\delta$ : 1.45 (s, 9H), 1.97 (d,  $J = 7.1$  Hz, 3H), 2.53 (t,  $J = 5.9$  Hz, 2H), 3.67 (q,  $J = 5.9$  Hz, 2H), 5.54 (q,  $J = 7.1$  Hz, 1H), 6.43 (s, 1H), 6.86 (t,  $J = 6.2$  Hz, 1H), 7.33 (t,  $J = 2.0$  Hz, 1H), 7.36 (d,  $J = 8.4$  Hz, 2H), 7.67 (d,  $J = 2.0$  Hz, 2H), 7.74 (d,  $J = 8.4$  Hz, 2H). MS C<sub>26</sub>H<sub>26</sub>Cl<sub>2</sub>F<sub>3</sub>N<sub>3</sub>O<sub>6</sub> calcd 635.09; obsd (M + Na) 657.89.

**N-[(4-[(1S)-1-[3-(3,5-Dichlorophenyl)-5-(6-methoxynaphthalen-2-yl)-1H-pyrazol-1-yl]ethyl]-phenyl)carbonyl]- $\beta$ -alaninate (9m).** *Step 1 (Method A).* Compound 8 (R = (S)-Me) (35 mg, 0.055 mmol), 6-methoxy-2-naphthylboronic acid (14 mg, 0.07 mmol), and TEA (42  $\mu\text{L}$ , 0.3 mmol) were dissolved in dimethoxyethane (1 mL)



and deoxygenated by vacuum-N<sub>2</sub> fill cycles. The catalyst Pd(PPh<sub>3</sub>)<sub>4</sub> (4 mg, 10% mol) was added, and the mixture was deoxygenated again before heated in microwave reactor to 100 °C for 10 min. The mixture was quenched with 4 mL of CH<sub>3</sub>CN–H<sub>2</sub>O (3:1, with 5% TFA) and product separated through reverse phase preparative HPLC. The collected product was treated with 1 mL of TFA–DCM (1:2) for 30 min and the residue lyophilized to give 30 mg (95%) of *N*-[4-((1*S*)-1-((3-(3,5-dichlorophenyl)-5-[6-methoxy-2-naphthyl]-1*H*-pyrazol-1-yl)ethyl)benzoyl]-β-alanine (**9m**) as a fine powder. <sup>1</sup>H NMR (500 MHz, DMSO-*d*<sub>6</sub>) δ: 1.90 (d, *J* = 7.0 Hz, 3H), 2.47 (t, *J* = 7 Hz, 2H), 3.41 (q, *J* = 7 Hz, 2H), 3.89 (s, 3H), 5.76 (q, *J* = 7.0 Hz, 1H), 7.16 (s, 1H), 7.20 (d, *J* = 8.4 Hz, 2H), 7.23 (dd, *J* = 2.6, 9.0 Hz, 1H), 7.39 (d, 2.6 Hz, 1H), 7.43 (dd, *J* = 1.7, 8.4 Hz, 1H), 7.56 (t, *J* = 1.9 Hz, 1H), 7.72 (d, *J* = 8.4 Hz, 2H), 7.83 (d, *J* = 9.0 Hz, 1H), 7.86 (d, *J* = 1.7 Hz, 1H), 7.91 (d, *J* = 8.4 Hz, 1H), 7.93 (d, *J* = 1.9 Hz, 2H), 8.44 (t, NH, *J* = 5.6 Hz, 1H). MS C<sub>32</sub>H<sub>27</sub>Cl<sub>2</sub>N<sub>3</sub>O<sub>4</sub> calcd 587.14; obsd (M + 1) 588.24.

***N*-[4-((1*S*)-1-[[3-(2,5-Dichlorophenyl)-5-(6-methoxynaphthalen-2-yl)-1*H*-pyrazol-1-yl]ethyl]phenyl)-carbonyl]-β-alanine (**15c**). Step 1.** A suspension of MgCl<sub>2</sub> (3.5 g, 35 mmol), potassium ethyl malonate (4.6 g, 30 mmol), and triethylamine (15 mL, 105 mmol) in dry ethyl acetate (100 mL) was stirred at 40 °C overnight. A suspension of 6-methoxynaphthyl-2-acid chloride (4.9 g, 22.2 mmol) in ethyl acetate (20 mL) was then added to the above mixture. The reaction was stirred at room temperature for 2.5 h. The reaction was quenched with 60 mL of 2N HCl, stirred for 5 min, and then washed with 0.5 N HCl twice, 5% K<sub>2</sub>CO<sub>3</sub> twice, and brine twice. Evaporation of solvent and vacuum drying afforded 6.0 g (98%) of ethyl 3-(6-methoxy-2-naphthyl)-3-oxopropanoate (**10**) as an oil. <sup>1</sup>H NMR (500 MHz, CDCl<sub>3</sub>) δ: 1.26 (t, *J* = 7.1 Hz, 3H), 3.95 (s, 3H), 4.09 (s, 2H), 4.23 (q, *J* = 7.1 Hz, 2H), 7.15 (d, *J* = 2.5 Hz, 1H), 7.21 (dd, *J* = 2.5 Hz, 9.0 Hz, 1H), 7.77 (d, *J* = 8.7 Hz, 1H), 7.85 (d, *J* = 9.0 Hz, 1H), 7.98 (dd, *J* = 1.8 Hz, 8.7 Hz, 1H), 8.38 (d, *J* = 1.8 Hz, 1H). About 10% of **10** existed in the enol and spectrum of the ketone form was reported.

**Step 2.** Compound **10** (5.0 g, 18.3 mmol) and anhydrous hydrazine (0.63 mL, 20 mmol) were refluxed in HOAc (100 mL) for 3 h. Solvent was removed under reduced pressure, and the residue was washed with DCM and collected by filtration to give 3.8 g (86%) of 5-(6-methoxy-2-naphthyl)-2,4-dihydro-3*H*-pyrazol-3-one (**11**) as an off-white solid. This compound exists in the hydroxypyrazole form in DMSO. <sup>1</sup>H NMR (500 MHz, DMSO-*d*<sub>6</sub>) δ: 3.87 (s, 3H), 5.95 (s, 1H), 7.17 (dd, *J* = 2.7 Hz, 9.0 Hz, 1H), 7.31 (d, *J* = 2.7 Hz, 1H), 7.74–7.84 (m, 3H), 8.11 (br s, 1H), 9.66 (br s, 1H), 12 (br, 1H). MS C<sub>14</sub>H<sub>12</sub>N<sub>2</sub>O<sub>2</sub> calcd 240.09; obsd (M + 1) 241.08.

**Step 3.** Compound **11** (1.58 g, 6.58 mmol) and pyridine (1.62 mL, 20 mmol) were dissolved in THF (20 mL) at –78 °C. Triflic anhydride (1.68 mL, 10 mmol) was added via syringe. The cooling bath was removed, and the reaction mixture was stirred for 2 h. The mixture was cooled down again to –78 °C and diluted with ethyl acetate (50 mL) and 2N HCl (10 mL). The ethyl acetate layer was washed with dilute HCl twice and brine twice. Evaporation of solvent left a purple residue, which was purified by column chromatography (SiO<sub>2</sub>, 0–2.5% ethyl acetate in DCM) to give 1.1 g (46%) of 3-(6-methoxy-2-naphthyl)-1*H*-pyrazol-5-yl trifluoromethanesulfonate (**12**) as a white solid. <sup>1</sup>H NMR (500 MHz, DMSO-*d*<sub>6</sub>) δ: 3.89 (s, 3H), 6.93 (d, *J* = 2.2 Hz, 1H), 7.23 (dd, *J* = 2.7 Hz, 8.8 Hz, 1H), 7.37 (d, *J* = 2.7 Hz, 1H), 7.82–7.86 (m, 2H), 7.92 (d, *J* = 8.7 Hz, 1H), 8.28 (s, 1H). MS C<sub>15</sub>H<sub>11</sub>F<sub>3</sub>N<sub>2</sub>O<sub>4</sub>S calcd 372.04; obsd (M + 1) 373.06.

**Step 4.** Compound **12** (1.36 g, 3.65 mmol), *tert*-butyl *N*-[4-(1-hydroxyethyl)benzoyl]-β-alanine (1.2 g, 4.02 mmol), and triphenylphosphine (1.44 g, 5.48 mmol) were suspended in DCM (25 mL). Diisopropyl azodicarboxylate (0.87 mL, 4.38 mmol) was added slowly. The mixture was stirred for 2 h and then concentrated to ~10 mL. This residue was chromatographed (SiO<sub>2</sub>, 25–30% ethyl acetate gradient) to give 0.73 g (31%) of *tert*-butyl *N*-[4-[1-(3-(6-methoxy-2-naphthyl)-5-[[trifluoromethyl]sulfonyl]oxy]-1*H*-pyrazol-1-yl)ethyl]benzoyl]-β-alanine (**14**) and 1.17 g (49%) of *tert*-butyl *N*-[4-[1-(5-(6-methoxy-2-naphthyl)-3-[[trifluoromethyl]sulfonyl]oxy]-1*H*-pyrazol-1-yl)ethyl]benzoyl]-β-alanine (**13**). Compound **14**: <sup>1</sup>H NMR (500 MHz, CDCl<sub>3</sub>) δ 1.45 (s, 9H), 2.01 (d, *J* = 7.1 Hz, 3H), 2.53 (t, *J* = 5.9 Hz, 2H), 3.67 (q, *J* = 5.9 Hz, 2H), 3.94 (s, 3H), 5.56 (q, *J* = 7.1

Hz, 1H), 6.54 (s, 1H), 6.78 (br, 1H), 7.16 (br, 1H), 7.17 (dd, *J* = 2.6 Hz, 9 Hz, 1H), 7.41 (d, *J* = 8.4 Hz, 2H), 7.74 (d, *J* = 8.4 Hz, 2H), 7.78 (d, *J* = 8.4 Hz, 1H), 7.79 (d, *J* = 8.5 Hz, 1H), 7.93 (dd, *J* = 1.8 Hz, 8.5 Hz, 1H), 8.14 (d, *J* = 1.6 Hz, 1H). MS C<sub>31</sub>H<sub>32</sub>F<sub>3</sub>N<sub>3</sub>O<sub>7</sub>S calcd 647.19; obsd (M + Na) 670.02. Compound **13**: <sup>1</sup>H NMR (500 MHz, CDCl<sub>3</sub>) δ 1.46 (s, 9H), 1.85 (d, *J* = 7.1 Hz, 3H), 2.55 (t, *J* = 5.8 Hz, 2H), 3.68 (q, *J* = 5.8 Hz, 2H), 3.95 (s, 3H), 5.52 (q, *J* = 7.1 Hz, 1H), 6.23 (s, 1H), 6.85 (br, 1H), 7.16 (d, *J* = 2.6 Hz, 1H), 7.21 (dd, *J* = 2.6 Hz, 8.7 Hz, 1H), 7.22 (d, *J* = 8.4 Hz, 2H), 7.24 (dd, *J* = 1.5 Hz, 8.4 Hz, 1H), 7.62 (d, *J* = 1.5 Hz, 1H), 7.67 (d, *J* = 8.7 Hz, 1H), 7.71 (d, *J* = 8.3 Hz, 2H), 7.76 (d, *J* = 8.4 Hz, 1H). MS C<sub>31</sub>H<sub>32</sub>F<sub>3</sub>N<sub>3</sub>O<sub>7</sub>S calcd 647.19; obsd (M + Na) 670.20.

**Step 5 (Method B).** Compound **13** (26 mg, 0.04 mmol), 2,5-dichlorophenylboronic acid (15 mg, 0.08 mmol), and PdCl<sub>2</sub>(dppf) (12 mg, 0.014 mmol) were suspended in toluene (0.6 mL) in a glass tube. A solution of Cs<sub>2</sub>CO<sub>3</sub> (5 M, 25 ul) was added. The mixture was deoxygenated by vacuum-N<sub>2</sub> fill cycles and heated in a microwave reactor to 140 °C for 10 min. The reaction mixture was filtered through a glass-fiber plug and solvent removed under reduced pressure. The residue was dissolved in CH<sub>3</sub>CN–H<sub>2</sub>O and purified by reverse phase preparatory HPLC. The intermediate ester thus obtained was deprotected by treatment with TFA–DCM (1:2, 1 mL) for 30 min. Evaporation of solvent and lyophilization from CH<sub>3</sub>CN–H<sub>2</sub>O yielded 6.4 mg (27%) of *N*-1-(4-(2-hydroxycarbonyl-ethylamino-carbonyl)phenyl)ethyl-3-(2,5-dichlorophenyl)-5-(6-methoxynaphth-2-yl)pyrazole (**15c(±)**) as a fine powder. <sup>1</sup>H NMR (500 MHz, DMSO-*d*<sub>6</sub>) δ: 1.90 (d, *J* = 6.9 Hz, 3H), 2.47 (t, *J* = 7.1 Hz, 2H), 3.41 (q, *J* = 7.1 Hz, 2H), 3.89 (s, 3H), 5.79 (q, *J* = 6.9 Hz, 1H), 7.02 (s, 1H), 7.22 (d, *J* = 8.4 Hz, 2H), 7.23 (d, *J* = 9.0 Hz, 1H), 7.39 (d, *J* = 2.6 Hz, 1H), 7.44 (dd, *J* = 1.7 Hz, 8.3 Hz, 1H), 7.47 (dd, *J* = 2.6 Hz, 8.6 Hz, 1H), 7.61 (d, *J* = 8.6 Hz, 1H), 7.74 (d, *J* = 8.4 Hz, 2H), 7.83 (d, *J* = 9.0 Hz, 1H), 7.88 (d, *J* = 1.7 Hz, 1H), 7.90 (d, *J* = 8.6 Hz, 1H), 7.92 (d, *J* = 2.6 Hz, 1H). MS C<sub>32</sub>H<sub>27</sub>Cl<sub>2</sub>N<sub>3</sub>O<sub>4</sub> calcd (M + H) 588.1451; obsd 588.1444.

Racemic *N*-[4-{1-[3-(2,5-dichlorophenyl)-5-(6-methoxy-2-naphthyl)-1*H*-pyrazol-1-yl]ethyl]benzoyl]-β-alanine was separated into its enantiomers by chromatography using a ChiralPak AS column (10 mm × 250 mm), eluting with 40% MeOH–CO<sub>2</sub> (0.1%TFA). Compound **15c** is the slower eluting enantiomer.

**Glucagon Binding Assay.** A CHO cell line expressing the human glucagon receptor (CHO hGCGR) was maintained and membranes prepared as described in Chicchi et al.<sup>42</sup> Membranes (2–5 μg) were incubated in buffer containing 50 mM Tris, pH 7.5, 5 mM MgCl<sub>2</sub>, 2 mM EDTA, 1% bovine serum albumin, 12% glycerol, 0.2 mg of wheat germ agglutinin-coated polyvinyltoluene scintillation proximity assay beads (Amersham Kit RPNP0001), increasing concentration of compound (diluted in 100% DMSO and added to the assay at a final concentration of 2.5%), and 50 pM <sup>125</sup>I-glucagon. The assay was incubated for 3 h at room temperature, and the total bound radioactivity was measured with a Wallac-Microbeta counter. Non-specific counts were determined using 1 μM unlabeled glucagon. Data were analyzed using the nonlinear regression analysis software GraphPad Prism, v4.

**cAMP Assay.** CHO hGCGR cells were grown in Iscove's Modified Dulbecco's Medium (IMDM), 10% FBS, 1 mM L-glutamine, penicillin–streptomycin (100 u/mL), and 500 ug G418/mL for 3–4 days before harvesting using Enzyme-Free Dissociation Media (EFD, Specialty Media). The cells were centrifuged at low speed and resuspended in stimulation buffer (FlashPlate, Perkin-Elmer, Kit SMP0004A). Compounds were diluted from DMSO stocks and added to the assay at a final concentration of 5% DMSO. Cells were preincubated with compound or DMSO controls for 30 min. Glucagon (250 pM) was added, and the samples were incubated at room temperature for an additional 30 min. The assay was terminated with the addition of the FlashPlate kit detection buffer. The assay was then incubated for an additional 3 h at room temperature, and bound radioactivity was measured using a liquid scintillation counter (TopCount-Packard Instruments). cAMP levels were determined as per manufacturer's instructions. For Schild Plot analysis, aliquots of cells were preincubated with 56, 100, 178, 300, 560, and 1000 nM **9m**

for 30 min at room temperature prior to the addition of 0.001–1000 nM glucagon to initiate the assay. Data were analyzed using the linear and nonlinear regression analysis software GraphPad Prism, v4.

Synthesis and characterization of other compounds listed in Tables 1 and 2 can be found in the Supporting Information.

## ■ ASSOCIATED CONTENT

### ■ Supporting Information

<sup>1</sup>H NMR spectra and MS spectra of compounds listed in Tables 1 and 2. Metabolism of compound **9m** in rat and dog. Acute efficacy study of **9m** in hGCGR ob/ob mice. Inhibition of glucagon-induced glycogenolysis in perfused hGCGR mouse liver. This material is available free of charge via the Internet at <http://pubs.acs.org>.

## ■ AUTHOR INFORMATION

### Corresponding Author

\*Phone: 1-732-594-7507. E-mail: [yusheng\\_xiong@merck.com](mailto:yusheng_xiong@merck.com).

### Notes

The authors declare no competing financial interest.

## ■ ACKNOWLEDGMENTS

We thank Dr. Charles W. Ross for determination of high-resolution mass spectra, Steve Mock for bioanalytical work, and Victor Ding and Edward Brady for their assistance in biological assays.

## ■ ABBREVIATIONS USED

GCGR, glucagon receptor; GIPR, glucose-dependent insulinotropic peptide receptor; PAC1, pituitary adenylate cyclase activating peptide receptor 1; VPAC1 and VPAC2, vasoactive intestinal peptide receptor 1 and 2; GRA, glucagon receptor antagonist; HbA1c, glycosylated hemoglobin

## ■ REFERENCES

- (1) (a) Zhang, B. B.; Moller, D. B. New approaches in the treatment of type 2 diabetes. *Curr. Opin. Chem. Biol.* **2000**, *4*, 461–467. (b) Jiang, G.; Zhang, B. B. Glucagon and regulation of glucose metabolism. *Am. J. Physiol.* **2003**, *284*, E671–E678. (c) Sloop, K. W.; Michael, D. D. Role of the glucagon receptor in glucose homeostasis: a therapeutic target to improve glycemic control in type 2 diabetes. *Drugs Future* **2004**, *29*, 835–841.
- (2) (a) Stumvoll, M.; Goldstein, B. J.; van Haefen, T. W. Type 2 diabetes: principles of pathogenesis and therapy. *Lancet* **2005**, *365*, 1333–1346. (b) Staehr, P.; Hother-Nielsen, O.; Beck-Nielsen, H. Hepatic glucose production: therapeutic target in type 2 diabetes? *Diabetes, Obes. Metab.* **2000**, *4*, 215–223. (c) Shah, P.; Vella, A.; Basu, A.; Basu, R.; Schwenk, W. F.; Rizza, B. A. Lack of Suppression of Glucagon Contributes to Postprandial Hyperglycemia in Subjects with Type 2 Diabetes Mellitus. *J. Clin. Endocrinol. Metab.* **2000**, *85*, 4053–4059.
- (3) DeFronzo, R. A. The Triumvirate: beta-cell, muscle, liver. A collusion responsible for NIDDM. *Diabetes* **1988**, *37*, 667–687.
- (4) (a) Brand, C. L.; Rolin, B.; Jorgensen, P. N.; Svendsen, I.; Kristensen, J. S.; Holst, J. J. Immunoneutralization of endogenous glucagon with monoclonal glucagon antibody normalizes hyperglycaemia in moderately streptozotocin-diabetic rats. *Diabetologia* **1994**, *37*, 985–993. (b) Sørensen, H.; Brand, D. L.; Neschen, S.; Holst, J. J.; Fosgerau, K.; Nishimura, E.; Gerald I. Shulman, D. L. Immunoneutralization of Endogenous Glucagon Reduces Hepatic Glucose Output and Improves Long-Term Glycemic Control in Diabetic ob/ob Mice. *Diabetes* **2006**, *55*, 2843–2848.
- (5) (a) Liang, Y.; Osborne, M. C.; Monia, B. P.; Bhanot, S.; Gaarde, W. A.; Reed, C.; She, P.; Jetton, T. L.; Demarest, K. T. Reduction in Glucagon Receptor Expression by an Antisense Oligonucleotide

Ameliorates Diabetic Syndrome in db/db Mice. *Diabetes* **2004**, *53*, 410–417. (b) Sloop, K. W.; Cao, J. X.-C.; Siesky, A. M.; Zhang, H. Y.; Bodenmiller, D. M.; Cox, A. L.; Jacobs, S. J.; Moyers, J. S.; Owens, R. A.; Showalter, A. D.; Brenner, M. B.; Raap, A.; Gromada, J.; Berridge, B. R.; Monteith, D. K. B.; Porsken, N.; McKay, R. A.; Monia, B. P.; Bhanot, S.; Watts, L. M.; Michael, M. D. Hepatic and glucagon-like peptide-1-mediated reversal of diabetes by glucagon receptor antisense oligonucleotide inhibitors. *J. Clin. Invest.* **2004**, *113*, 1571–1581.

(6) (a) Johnson, D. G.; Goebel, C. U.; Hrubby, V. J.; Bregman, M. D.; Trivedi, D. Hyperglycemia of Diabetic Rats Decreased by a Glucagon Receptor Antagonist. *Science* **1982**, *215*, 1115–1116. (b) Ahn, J. M.; Medeiros, M.; Trivedi, D.; Hrubby, V. J. Development of Potent Truncated Glucagon Antagonists. *J. Med. Chem.* **2001**, *44*, 1372–1379.

(7) (a) Sloop, K. W.; Michael, M. D.; Moyers, J. S. Glucagon as a target for the treatment of Type 2 diabetes. *Expert Opin. Ther. Targets* **2005**, *9* (3), 593–600. (b) Kurukulasuriya, R.; Link, J. T. Progress towards glucagon receptor antagonist therapy for Type 2 diabetes. *Expert Opin. Ther. Pat.* **2005**, *15* (12), 1739–1749.

(8) DeMong, D. E.; Miller, M. W.; Lachowicz, J. E. Glucagon Receptor Antagonists for Type II Diabetes. *Annu. Rep. Med. Chem.* **2008**, *43*, 119–137. For an earlier review see (b) Ling, A. Small molecule glucagon receptor antagonists. *Drugs Future* **2002**, *27* (10), 987–993.

(9) Collins, J. L.; Dambek, P. J.; Goldstein, S. W.; Faraci, W. S. CP-99711: a non-peptide glucagon receptor antagonist. *Bioorg. Med. Chem. Lett.* **1992**, *9*, 915–918.

(10) Madsen, P.; Knudsen, L. B.; Wiberg, F. C.; Carr, R. D. Discovery and Structure–Activity Relationship of the First Non-Peptide Competitive Human Glucagon Receptor Antagonists. *J. Med. Chem.* **1998**, *41*, 5150–5157.

(11) de Laszlo, S. E.; Hacker, C.; Li, B.; Kim, D.; MacCoss, M.; Mantlo, N.; Pivnichny, J. V.; Colwell, L.; Koch, G. E.; Cascieri, M. A.; Hagmann, W. K. Potent, orally absorbed glucagon receptor antagonists. *Bioorg. Med. Chem. Lett.* **1999**, *9*, 641–646.

(12) (a) Ling, A.; Hong, Y.; Gonzalez, J.; Gregor, V.; Polinsky, A.; Kuki, A.; Shi, S.; Teston, K.; Murhpy, D.; Porter, J.; Kiel, D.; Lakis, J.; Anderes, K.; May, J. Identification of alkylidene hydrazide as glucagon receptor antagonists. *J. Med. Chem.* **2001**, *44*, 3141–3149. (b) Madsen, P.; Ling, A.; Plewe, M.; Sams, C. K.; Knudsen, L. B.; Sedelmann, U. G.; Ynddal, L.; Brand, C. L.; Andersen, B.; Murphy, D.; Teng, M.; Truesdale, L.; Diel, D.; May, J.; Kuki, A.; Shi, S.; Johnson, M. D.; Teston, K. A.; Feng, J.; Lakis, J.; Anderes, K.; Gregor, V.; Lau, J. Optimization of alkylidene hydrazide based human glucagon receptor antagonists. Discovery of the highly potent and orally available 3-cyano-4-hydroxybenzoic acid [1-(2,3,5,6-tetramethylbenzyl)-1H-indol-4-ylmethylene]hydrazide. *J. Med. Chem.* **2002**, *45*, 5755–5775.

(13) Fujii, A.; Negoro, T.; Migihashi, C.; Murata, M.; Nakamura, K.; Nukuda, T.; Matsumoto, T.; Konno, K. 2-furancarboxylic acid hydrazides and pharmaceutical compositions containing the same. WO Patent 064404, 2003.

(14) Duffy, J. L.; Kirk, B. A.; Konteatis, Z.; Campbell, E. L.; Liang, R.; Brady, E. J.; Candelore, M. R.; Ding, V. D. H.; Jiang, G.; Liu, F.; Qureshi, S. A.; Saperstein, R.; Szalkowski, D.; Sharon Tong, S.; Tota, L. M.; Xie, D.; Yang, X.; Zafian, P.; Zheng, S.; Chapman, K. T.; Zhang, B. B.; Tata, J. R. Discovery and investigation of a novel class of thiophene-derived antagonists of the human glucagon receptor. *Bioorg. Med. Chem. Lett.* **2005**, *15*, 1401–1405.

(15) (a) Ladouceur, G. H.; Cook, J. H.; Doherty, E. M.; Schoen, W. R.; MacDougall, M. L.; Livingston, J. N. Discovery of 5-hydroxy-4-phenylpyridines as a new class of glucagon receptor antagonists. *Bioorg. Med. Chem. Lett.* **2002**, *12*, 461–464. (b) Smith, A. R.; Hertzog, D. L.; Osterhout, M. H.; Ladouceur, G. H.; Korpusik, M.; Bobko, M. A.; Jones, J. H.; Phelan, K.; Romero, R. H.; Hundertmark, T.; MacDougall, M. L.; Livingston, J. N.; Schoen, W. R. Optimization of the 4-aryl group of 4-aryl-pyridine glucagon antagonists: development of an efficient, alternative synthesis. *Bioorg. Med. Chem. Lett.* **2002**, *12*, 1303–1306. (c) Ladouceur, G. H.; Cook, J. H.; Hertzog, D. L.; Jones, J. H.; Hundertmark, T.; Korpusik, M.; Lease, T. G.; Livingston, J. N.; MacDougall, M. L.; Osterhout, M. H.; Phelan, K.; Romero, R. H.;

- Schoen, W. R.; Shao, C.; Smith, R. Integration of optimized substituted patterns to produce highly potent 4-aryl-pyridine glucagon receptor antagonists. *Bioorg. Med. Chem. Lett.* **2002**, *12*, 3421–3424.
- (d) Petersen, K. F.; Sullivan, J. T. Effects of a novel glucagon receptor antagonist (Bay 27-9955) on glucagon-stimulated glucose production in humans. *Diabetologia* **2001**, *44*, 2018–2024.
- (16) (a) Ling, A.; Plewe, M. B.; Truesdale, L. K.; Lau, J.; Madsen, P.; Sams, C. J.; Dehrens, C.; Vagner, J.; Christensen, I. T.; Lundt, B. F.; Sidelmann, U. G.; Thøgersen, H. Glucagon antagonist/inverse agonist. WO 2000/069810, 2000. (b) Lau, J.; Behrens, C.; Sidelmann, U. G.; Knudsen, L. B.; Lundt, B.; Sams, C.; Ynddal, L.; Brand, C. L.; Pridal, L.; Ling, A.; Kiel, D.; Plewe, M.; Shi, S.; Madsen, P. New  $\beta$ -alanine derivatives are orally available glucagon receptor antagonists. *J. Med. Chem.* **2007**, *50* (1), 113–128. (c) Kodra, J. T.; Jørgensen, A. S.; Andersen, B.; Behrens, C.; Brand, C. L.; Christensen, I. T.; Guldbrandt, M.; Jeppesen, C. B.; Knudsen, L. B.; Madsen, P.; Nishimura, E.; Sams, C.; Sidelmann, U. G.; Pedersen, R. A.; Lynn, F. C.; Lau, J. Novel Glucagon Receptor Antagonists with Improved Selectivity over the Glucose-Dependent Insulinotropic Polypeptide Receptor. *J. Med. Chem.* **2008**, *51* (17), 5387–5396.
- (17) Madsen, P.; Kodra, J. T.; Behrens, C.; Nishimura, E.; Jeppesen, C. B.; Pridal, L.; Andersen, B.; Knudsen, L. B.; Valcace-Aspegren, C.; Guldbrandt, M.; Christensen, I. T.; Jørgensen, A. S.; Ynddal, L.; Brand, C. L.; gagger, M. A.; Lau, J. Human glucagon receptor antagonists with thiazole cores. A novel series with superior pharmacokinetic properties. *J. Med. Chem.* **2009**, *52*, 2989–3000.
- (18) Rivera, N.; Everett-Grueter, C. A.; Edgerton, C. S.; Rodewald, T.; Neal, D. W.; Nishimura, E.; Larsen, M. O.; Jacobsen, L. O.; Kristensen, K.; Brand, C. L.; Cherrington, A. D. A Novel Glucagon Receptor Antagonist, NNC 25-0926, Blunts Hepatic Glucose Production in the Conscious Dog. *J. Pharm. Exp. Ther.* **2007**, *321* (2), 743–752.
- (19) Shen, D.; Lin, S.; Parmee, E. R. A survey of small molecule glucagon receptor antagonists from recent patents (2006–2010). *Expert Opin. Ther. Pat.* **2011**, *21* (8), 1211–1240.
- (20) Filipski, K. J.; Bian, J.; Ebner, D. C.; Lee, E. C. Y.; Li, J.-C.; Sammons, M. F.; Wright, S. W.; Stevens, B. D.; Didiuk, M. T.; Tu, M.; Perreault, C.; Brown, J.; Atkinson, K.; Tan, B.; Salatto, C. T.; Litchfield, J.; Pfefferkorn, J. A.; Guzman-Perez, A. A novel series of glucagon receptor antagonists with reduced molecular weight and lipophilicity. *Bioorg. Med. Chem. Lett.* **2012**, *22*, 415–420.
- (21) (a) Kelly, R. P.; Garhyan, P.; Abu-Raddad, E. J.; Fu, H.; Lim, G. N.; Prince, M. J.; Pinare, J. A.; Loh, M. T.; Deeg, M. A. Short-Term Treatment with Glucagon Receptor Antagonist LY2409021 Effectively Reduces Fasting Blood Glucose (FBG) and HbA1c in Patients with Type 2 Diabetes Mellitus (T2DM). ADA Scientific Session, San Diego, 2011. *Diabetes* **2011**, *60* (supplement\_1), A84. (b) Conner, S. E.; Zhu, G. Glucagon receptor antagonists, preparation and therapeutic uses. US Patent 7816557, 2010. (c) Conner, S. E.; Zhu, G.; Li, J. Glucagon receptor antagonists, preparation and therapeutic uses. US Patent 0124648, 2011. (d) Conner, S. E.; Zhu, G.; Li, J. Glucagon receptor antagonists, preparation and therapeutic uses. US Patent 0324140, 2010.
- (22) Shen, D. M.; Brady, E. J.; Candelore, M. R.; Dallas-Yang, Q.; Ding, V. D.-H.; Jiang, G.; McCann, P. E.; Mock, S.; Quresh, S. A.; Saperstein, R.; Tong, X.; Tota, L. M.; Wright, M. J.; Yang, X.; Zheng, S.; Chapman, K. T.; Zhang, B. B.; Tata, J. R.; Parmee, E. R. Discovery of novel, selective and orally active human glucagon receptor antagonists containing a pyrazole core. *Bioorg. Med. Chem. Lett.* **2011**, *21*, 76–81.
- (23) Kurukulasuriya, R.; Sorensen, B. K.; Link, J. T.; Patel, J. R.; Jae, H.-S.; Winn, M. X.; Rohde, R. R.; Grihalde, N. D.; Lin, C. W.; Ogiela, C. A.; Adler, A. L.; Collins, C. A. Biaryl amide glucagon receptor antagonist. *Bioorg. Med. Chem. Lett.* **2004**, *14* (9), 2047–2050.
- (24) Kim, R. M.; Chang, J.; Lins, A. R.; Brady, E.; Candelore, M. R.; Dallas-Yang, Q.; Ding, V.; Dragovic, J.; Iliff, S.; Jiang, G.; Mock, S.; Qureshi, S.; Saperstein, R. S.; Szalkowski, D.; Tamvakopoulos, C.; Tota, L.; Wright, M.; Yang, X.; Tata, J. R.; Chapman, K.; Zhang, B. B.; Parmee, E. R. Discovery of potent, orally active benzimidazole glucagon receptor antagonists. *Bioorg. Med. Chem. Lett.* **2008**, *18*, 3701–3705.
- (25) Wang, X.-J.; Tan, J.; Grozinger, K. Cross-coupling of 1-aryl-5-bromopyrazoles: regioselective synthesis of 3,5-disubstituted 1-arylpzrazoles. *Tetrahedron Lett.* **2000**, *41*, 4713–4716.
- (26) Clay, R. J.; Collum, T. A.; Karrick, G. L.; Wemple, J. A Safe, Economical Method for the Preparation of  $\beta$ -Oxo Esters. *Synthesis* **1993**, 290–292.
- (27) (a) Grimmett, M. R.; Lim, K. H. R.; Weavers, R. T. The *N*-Alkylation and *N*-Arylation of Unsymmetrical Pyrazoles. *Aust. J. Chem.* **1979**, *32*, 2203–2213. (b) Guillou, S.; Bonhomme, F. J.; Janin, Y. L. Nitrogen's reactivity of various 3-alkoxy-pyrazoles. *Tetrahedron* **2009**, *65*, 2660–2668.
- (28) Goikhman, R.; Jacques, T. L.; Sames, D. C–H Bonds as Ubiquitous Functionality: A General Approach to Complex Arylated Pyrazoles via Sequential Regioselective C-Arylation and N-Alkylation Enabled by SEM-Group Transposition. *J. Am. Chem. Soc.* **2009**, *131* (8), 3042–3048.
- (29) Burk, M. J.; Martinez, J. P.; Feaster, J. E.; Cosford, N. Catalytic asymmetric reductive amination of ketones via highly enantioselective hydrogenation of the C=N double bond. *Tetrahedron* **1994**, *50* (15), 4399–4428.
- (30) Yoshikawa, N.; Tan, L.; McWilliams, J. C.; Ramasamy, D.; Sheppard, R. Catalytic Enantioselective Hydrogenation of *N*-Alkoxy-carbonyl Hydrazones: A Practical Synthesis of Chiral Hydrazines. *Org. Lett.* **2010**, *12* (2), 276–279.
- (31) Schlosser, M.; Castagnetti, E. 1,2-Didehydro-3- and -4-(Trifluoromethoxy)benzene: The “Aryne” Route to 1- and 2-(Trifluoromethoxy)naphthalenes. *Eur. J. Org. Chem.* **2001**, 3991–3997.
- (32) Liang, R.; Abrardo, L.; Brady, E. J.; Candelore, M. R.; Ding, V.; Saperstein, R.; Tota, L. M.; Wright, M.; Mock, S.; Tamvakopoulos, C.; Tong, X.; Zheng, S.; Zhang, B. B.; Tata, J. R.; Parmee, E. R. Design and synthesis of conformationally constrained tri-substituted ureas as potent antagonists of the human glucagon receptor. *Bioorg. Med. Chem. Lett.* **2007**, *17*, 587–592.
- (33) Mu, J.; et al. Manuscript in preparation.
- (34) Functional assays (cAMP measurement) for the selected family B GPCR were carried out in the similar conditions as for GCGR, with human receptors GLP-1R, GIPR, and VPACR2 expressed in CHO cells, and PAC1 expressed in HIN 3T3 cells, and VPAC1 in HT29 cells.
- (35) (a) Lynch, J. J.; Wallace, A. A.; Stupinski, R. F.; Baskin, E. P.; Beare, C. M.; Appleby, S. D.; Salata, J. J.; Jurkiewicz, N. K.; Sanguinetti, M. C.; Stein, R. B. Cardiac electrophysiologic and antiarrhythmic actions of two long-acting spirobenzopyran piperidine class III agents, L-702,958 and L-706,000 [MK-499]. *J. Pharmacol. Exp. Ther.* **1994**, *269*, 541–554. (b) Schoemaker, H.; Hicks, P.; Langer, S. Calcium Channel Receptor Binding Studies for Diltiazem and Its Major Metabolites: Functional Correlation to Inhibition of Portal Vein Myogenic Activity. *J. Cardiovasc. Pharm.* **1987**, *9*, 173–180. (c) Hartmann, H. A.; Tiedeman, A. A.; Chen, S. F.; Brown, A. M.; Kirsch, G. E. Effects of III–IV Linker Mutations on Human Heart Na<sup>+</sup> Channel Inactivation Gating. *Circ. Res.* **1994**, *75*, 114–122.
- (36) Qureshi, S. A.; Candelore, M. R.; Xie, D.; Yang, X.; Tota, L. M.; Ding, V. D.; Li, Z.; Bansal, A.; Miller, C.; Cohen, S. M.; Jiang, G.; Brady, E.; Saperstein, R.; Duffy, J. L.; Tata, J. R.; Chapman, K. T.; Moller, E. D.; Zhang, B. B. A novel glucagon receptor antagonist inhibits glucagon-mediated biological effects. *Diabetes* **2004**, *53*, 3267–3273.
- (37) Cohen, M. S.; Werrmann, J. G.; Tota, M. R. <sup>13</sup>C NMR study of the effects of leptin treatment on kinetics of hepatic intermediary metabolism. *Proc. Natl. Acad. Sci. U.S.A.* **1998**, *95* (13), 7385–7390.
- (38) Cohen, S. M.; Duffy, J. L.; Miller, C.; Kirk, B. A.; Candelore, M. R.; Rios, M.; Ding, V. D. H.; Kaczorowski, G.; Tota, L. M.; Werrmann, J. G.; Wright, M.; Parmee, E. R.; Tata, J. R.; Zhang, B. B. Direct observation (NMR) of the efficacy of glucagon receptor antagonists in murine liver expressing the human glucagon receptor. *Bioorg. Med. Chem.* **2006**, *14*, 1506–1517.

(39) Mu, J.; Jiang, G.; Brady, E.; Dallas-Yang, Q.; Liu, F.; Woods, J.; Zycband, E.; Wright, M.; Li, Z.; Lu, K.; Zhu, L.; Shen, X.; SinhaRoy, R.; Candelore, M. L.; Qureshi, S. A.; Shen, D.-M.; Zhang, F.; Parmee, E. R.; Zhang, B. B. Chronic treatment with a glucagon receptor antagonist lowers glucose and moderately raises circulating glucagon and glucagon-like peptide 1 without severe alpha cell hypertrophy in diet-induced obese mice. *Diabetologia* **2011**, *54* (9), 2381–2391.

(40) (a) Gelling, R. W.; Du, X. Q.; Dichmann, D. S.; Romer, J.; Huang, H.; Cui, L.; Obici, S.; Tang, B.; Holst, J. J.; Fledelius, C.; Johansen, R. B.; Rossetti, L.; Jelicks, L. A.; Serup, P.; Nishimura, E.; Charron, M. J. Lower blood glucose, hyperglucagonemia, and pancreatic a cell hyperplasi in glucagon receptor knockout mice. *Proc. Natl. Acad. Sci. U.S.A.* **2003**, *100*, 1438–1443. (b) Sorensen, H.; Winzell, M. S.; Brand, C. L.; Fosgerau, K.; Gelling, R. W.; Nishimura, E.; Ahren, Bo. Glucagon Receptor Knockout Mice Display Increased Insulin Sensitivity and Impaired  $\beta$ -Cell Function. *Diabetes* **2006**, *55*, 3463–3469.

(41) (a) Parmee, E. R. Discovery of MK-0893: a glucagon receptor antagonist for the treatment of type II diabetes. 241st ACS National Meeting and Exposition, Anaheim, CA, March 27–31, 2011, MEDI-31. (b) Engel, S. S.; Xu, L.; Andryuk, P. J.; Davies, M. J.; Amatruda, J.; Kaufman, K.; Goldstein, B. J. Efficacy and Tolerability of MK-0893, a Glucagon Receptor Antagonist (GRA), in Patients with Type 2 Diabetes (T2DM). ADA Scientific Session, San Diego, 2011. *Diabetes* **2011**, *60* (supplement\_1), A85. (c) Ruddy, M.; Pramanik, B.; Luncford, S. L.; Cilissen, C.; Stoch, A.; Wagner, J.; Amatruda, J.; Herman, G.; Kaufman, K. Inhibition of Glucagon-Induced Hyperglycemia Predicts Glucose Lowering Efficacy of a Glucagon Receptor Antagonist, MK-0893, in Type 2 Diabetes (T2DM). ADA Scientific Session, San Diego, 2011. *Diabetes* **2011**, *60* (supplement\_1), A85.

(42) Chicchi, G. G.; Graziano, M. P.; Koch, G.; Hey, P.; Sullivan, K.; Vicario, P. P.; Cascieri, M. A. Alterations in Receptor Activation and Divalent Cation Activation of Agonist Binding by Deletion of Intracellular Domains of the Glucagon Receptor. *J. Biol. Chem.* **1997**, *272*, 7765–7769.